Animal Behaviour 159 (2020) 105–119

Contents lists available at ScienceDirect

Animal Behaviour

journal homepage: www.elsevier.com/locate/anbehav

Environmental and genetic constraints on cuticular hydrocarbon composition and nestmate recognition in ants

Irene Villalta [a, b, *], Léa Rami [a, b], Paloma Alvarez-Blanco [a], Elena Angulo [a], Xim Cerdá [a], Raphaël Boulay [b]

[a] Estación Biológica de Doñana, CSIC, Sevilla, Spain
[b] Institute of Insect Biology, University François Rabelais of Tours, Tours, France

ARTICLE INFO

Article history:
Received 12 April 2019
Initial acceptance 5 July 2019
Final acceptance 14 October 2019

MS. number: 19-00264R

Keywords:
ants
chemical communication
cuticular hydrocarbons
elevational gradient
intraspecific aggression
nestmate recognition
resistance to desiccation

In insects, cuticular hydrocarbon (CHC) profiles are complex phenotypic traits with several functions: they provide protection against pathogens and water loss and convey information about insect identity. They are particularly important in ants as they are the basis for colony-specific signatures, which allow nestmate recognition and thus help colonies protect their resources from competitors. Several studies have shown that levels of n-alkanes are strongly influenced by the environment and that, alongside methyl-branched alkanes, n-alkanes are involved in various signalling tasks. Here, we analysed the CHCs of the ant *Aphaenogaster iberica* along an elevational gradient running from sea level to 2000 m. Across this gradient, we found a considerable difference in mean daily temperature of more than 10 °C between the populations on either end of the gradient as well as a marked degree of genetic structuring among populations. Moreover, genetic distance between populations increased with elevational distance but was independent of horizontal distance. Low-elevation populations had larger amounts of heavier compounds, including nonacosane (C29), and smaller amounts of lighter compounds, including hexacosane (C26) and heptacosane (C27). The level of aggression among non-nestmates increased with elevational distance, horizontal distance and CHC dissimilarity. However, mean within-population aggression (i.e. among colonies of the same population) did not differ across elevation. We also found that aggression was related to CHC levels: the correlation between the level of aggression and CHC dissimilarity remained significant even after we accounted for the correlation between genetic distance and aggression. We propose that climatic differences at different elevations may constrain CHC diversity and, consequently, the process of nestmate recognition.

Arthropod cuticular hydrocarbons (CHCs) are one of the best examples of a complex phenotypic trait with multiple functions (Menzel, Blaimer, & Schmitt, 2017; Menzel, Zumbusch, & Feldmeyer, 2018). The primary function of CHCs is to limit cuticular transpiration and thus maintain water balance. These compounds have probably played a decisive role in allowing arthropods to colonize terrestrial habitats (Jallon & David, 1987). In insects, most CHCs are 17–49 carbons long and display variable degrees of saturation and methylation (Morgan, 2004). It has been suggested that linear alkanes (i.e. *n*-alkanes) may provide greater resistance to desiccation and/or high temperatures than do methylated and unsaturated CHCs. Hence, cuticular hydrophobicity is tightly linked to hydrocarbon melting point (Gibbs & Rajpurohit, 2010). As ambient temperature increases, the CHC layer becomes less viscous, which reduces its waterproofing capacity. For a given carbon-chain length, the melting point is several degrees Celsius higher for *n*-alkanes than for methyl-branched alkanes and alkenes (Gibbs, 1995; Gibbs & Pomonis, 1995). Thus, *n*-alkanes are likely to provide better resistance to desiccation, especially at high temperatures, than do methyl-branched alkanes and alkenes (Hadley, 1978; Johnson & Gibbs, 2004; Rourke, 2000; Sprenger, Burkert, Abou, Federle, & Menzel, 2018; Toolson, 1982; Toolson & Hadley, 1979).

Various studies have shown that CHC composition, particularly that of *n*-alkanes, varies along aridity and temperature gradients within species or between closely related species (Frentiu & Chenoweth, 2010; Menzel et al., 2018, 2017; Rajpurohit et al., 2017; Rouault, Capy, & Jallon, 2000; Rourke, 2000). These differences might be due to a response to stressful conditions, where CHC

* Correspondence: I. Villalta, Institute of Insect Biology, University François Rabelais of Tours, Parc de Grandmont, Tours, 37200, France.
E-mail address: irenevillaltaalonso@gmail.com (I. Villalta).

https://doi.org/10.1016/j.anbehav.2019.11.008
0003-3472/

synthesis is adjusted via phenotypic plasticity rather than alterations in a population's genetic background (Gibbs, Louie, & Ayala, 1998). Alternatively, differential selection pressures along environmental gradients may promote specific adaptations to local conditions (Dudaniec, Yong, Lancaster, Svensson, & Hansson, 2018). Such responses arise across generations and are induced by genetic modifications. However, an important prerequisite to local adaptation is constrained gene flow among populations (Kawecki & Ebert, 2004). Hence, even if there are strong genetic underpinnings and directional selection on certain traits like CHCs, immigration may constantly move the average phenotype away from its optimal value, generating a mismatch with environmental conditions (Alcántara et al., 2007; Thompson, 1999). Nevertheless, steep selection gradients among populations may also reduce the success of immigrants if the latter are less suited to local conditions than are residents (Nosil, 2012; Räsänen & Hendry, 2008). Therefore, once local adaptation has occurred, it may also increase genetic isolation among populations.

In many insect species, including ants, the second function of CHCs is to convey information about reproductive status, immunological state and group or species identity (Blomquist & Bagnères, 2010; Villalta, Abril, Cerdá, & Boulay, 2018). Some studies suggest that, owing to their greater structural diversity, branched compounds may be particularly useful for communicating complex messages (Guerrieri et al., 2009; Martin & Drijfhout, 2009). However, this notion was recently challenged by the observation that some ants use single *n*-alkanes as pheromones (Van Oystaeyen et al., 2014). An important context in which ants use CHCs is nestmate recognition (Bonavita-Cougourdan, Clément, & Lange, 1987; Guerrieri et al., 2009; Lahav, Soroker, Hefetz, & Vander Meer, 1999; Martin, Vitikainen, Helanterä, & Drijfhout, 2008; Wagner, Tissot, Cuevas, & Gordon, 2000). To protect their colonies from competitors, workers compare the CHC profiles of individuals they encounter with an internal template of their colony's odour (D'Ettorre & Lenoir, 2010). Unfamiliar signals generate aggression while familiar ones do not. Although the behavioural response is bimodal (aggression or not), the probability that a signalling difference triggers antagonism may depend on the degree of chemical dissimilarity between individuals (Lenoir, Fresneau, Errard, & Hefetz, 1999; Sturgis & Gordon, 2012). Therefore, efficient nestmate recognition relies on CHC homogeneity within colonies and CHC dissimilarity between colonies (Boulay, Cerdá, Simon, Roldan, & Hefetz, 2007).

Indirect evidence suggests CHCs are highly heritable in ants and other insect taxa (Martin, Vitikainen, Shemilt, Drijfhout, & Sundström, 2013; Obin & Vander Meer, 1988; Provost, 1991; Sharma, Mitchell, Hunt, Tregenza, & Hosken, 2012; Wicker-Thomas & Chertemps, 2010; Zweden, Dreier, & Ettorre, 2009). However, genetic differences may be attenuated by environmental factors (Sprenger et al., 2018), such as the nesting material used, the types of food consumed and even rearing temperatures (Gibbs et al., 1998; Liang & Silverman, 2000; Rajpurohit et al., 2017; Wagner, Tissot, & Gordon, 2001). Frequent social interactions among nestmates contribute to the constant exchange of genetically and environmentally determined CHCs, which creates a Gestalt colony odour borne and recognized by all nestmates (Boulay, Hefetz, Soroker, & Lenoir, 2000; Boulay, Katzav-Gozansky, Hefetz, & Lenoir, 2004; Crozier & Dix, 1979; Dahbi, Hefetz, Cerdá, & Lenoir, 1999; Soroker, Vienne, & Hefetz, 1995). However, nestmate recognition may not function properly if CHC dissimilarity between colonies is low, a situation that can arise if colonies face similar environmental constraints and/or display low genetic diversity due to limited dispersal capacities.

In this study, we aimed to investigate potential constraints on nestmate recognition induced by environmental and genetic conditions. In this context, *Aphaenogaster iberica* is a good model species because it is found along an elevational gradient spanning over 2000 m, where populations on either end of the gradient experience a difference in mean daily temperature of more than 10 °C. Moreover, it is a strictly diurnal thermophilic species that must deal with daily variation in temperature while foraging. Finally, colonies are formed by fission, a system in which young mated queens leave the mother nest on foot to found new colonies a few metres away. As in the congeneric species *Aphaenogaster senilis*, frequent nest relocations limit isolation by distance between colonies at the local scale (Galarza et al., 2012). However, the high level of genetic isolation among populations resulting from limited female dispersal could be partially compensated for by male gene flow (females are wingless, but males do have wings and can fly).

First, we analysed variation in *A. iberica* CHCs along an elevational gradient. In contrast to the many studies that have examined the relative abundance of CHCs, our study adopted a more quantitative approach. If CHC production is costly, we would expect ants at higher elevations to produce smaller absolute quantities of CHCs and, more specifically, of *n*-alkanes: because they are not exposed to high environmental temperatures, they should not need the protection afforded by CHCs. Moreover, we expected distance between populations to correlate negatively with CHC profile similarity: neighbouring populations should have more similar CHC profiles because they experience similar abiotic conditions and are more genetically similar. We also used mitochondrial and microsatellite markers to evaluate the degree of genetic isolation among populations. We expected that the level of genetic isolation would increase with elevation. In contrast, we predicted that genetic diversity would decrease with elevation because ants rarely immigrate to higher elevations, a situation that could promote local adaptation. Finally, we tested whether the degree of nestmate recognition among colonies within populations varied with elevation given that CHC diversity was expected to decline with elevation. Moreover, we expected the degree of nestmate recognition among populations to correlate with geographical distance, genetic distance and CHC similarity.

METHODS

Study Site and Sampling

We sampled eight populations (Z100, Z150, Z300, Z600, Z1000, Z1300, Z1700 and Z2000) along an elevational gradient in the Sierra Nevada mountain range near the village of Lanjarón, Spain (36.91°N, 3.47°W). The locations of all the colonies in this study were determined using a Leica GPS1200; we corrected the measurements using the reference station in the town of Motril. The horizontal distance between the lowest and highest populations was 30 km. The low-elevation populations (Z100–Z600) were not directly affected by human disturbance but were surrounded by greenhouses and orchards (Fig. A1). The mid-elevation populations (Z1000 and Z1300) were in a zone with mixed vegetation and scattered pine trees. The high-elevation populations (Z1700 and Z2000) were in an area that had experienced a wildfire in 2005 that destroyed all the trees found there. After the fire, the burned wood was left in place, and no trees were replanted. When we carried out our study, in 2015, the vegetation was still exclusively composed of herbaceous plants.

The ants used in the chemical and behavioural analyses were kept under controlled conditions (25 °C) for 8 months. During this period, they lived in plastic boxes (20 x 15 cm and 12 cm high), whose inner walls had been coated with Fluon to prevent the ants from escaping. For shelter, they were given one or two 20 x 2 cm test tubes that were half filled with water plugged with cotton

wool. They also had ad libitum access to food (dead mealworms, *Tenebrio molitor*, and pieces of fruit).

Cuticular hydrocarbon analysis

In the field, we collected 198 fragments of colonies (23–27 per population), each comprising 100–1000 workers. We performed the CHC extractions after the ants had spent 8 months in the laboratory to reduce the potential effects of environmental differences on CHC levels; we did not want to wait too long because workers live only 1–2 years in the laboratory. We prepared one CHC sample per colony by immersing the thoraces and legs of three randomly chosen ants in 100 μl of hexane for 1 h; the hexane contained 20 ng of eicosane as an internal standard. The ants had previously been killed by freezing (-18 °C for 10 min). After the extraction process, the thoraces and legs were placed in alcohol until measurements of tibia length could be carried out using the Image J software (Schneider, Rasband, & Eliceiri, 2012).

We injected 1 μl of each sample into a gas chromatograph–mass spectrometer (GC–MS; an Agilent 7890A GC coupled with a 7000C Triple Quadrupole GC/MS; Agilent Technologies, Santa Clara, CA, U.S.A.) equipped with an HP-5MS fused silica capillary column (30 m × 250 μm × 0.25 μm) with a splitless time of 2 min at 250 °C. Oven temperature was programmed to rise from 150 °C (2 min initial hold) to 320 °C at a speed of 5 °C/min (5 min final hold). Eluted compounds were then identified (ionization voltage: 70eV; scan mode: 40–550 amu). Fragments were analysed using MassHunter Qualitative Analysis v. B.06.00 (Agilent Technologies) and compared with those in published sources.

Sampling, Extraction, and Amplification of Genetic Material

For the genetic analyses, we sampled one worker from 25–32 colonies per population (total of 235 colonies, which included the 198 colony fragments used for the CHC analyses); the coordinates of the sampling sites and the NCBI sequence accession numbers are listed in Table A1. The workers were collected in the field and immediately individually stored in 96% ethanol. DNA was extracted from the thorax and legs of one worker per colony using the Wizard Genomic DNA Purification Kit (Promega, Madison, WI, U.S.A.). A 1034-bp sequence of the mitochondrial cytochrome oxidase subunit I (COI) was amplified from each sample using the primers described in the Appendix. We then performed polymerase chain reaction (PCR) analysis: the reaction volume was 30 μl (1 μl of extracted DNA, 1.5 μl of each primer [20 mM], 15 μl of HotStarTaq Master Mix Kit [Qiagen, Hilden, Germany] and 11 μl of nuclease-free water). PCR amplification comprised an initial denaturation step at 95 °C (15 min), which was followed by 35 cycles at 94 °C (45 s), annealing temperature (1 min) and 72 °C (1 min 30 s) and, finally, by an extension step at 72 °C (10 min). The PCR templates were purified with the NucleoSpin Gel and PCR Clean-up Kit (Macherey-Nagel, Düren, Germany) and were sequenced using an automated ABI 3730XL sequencer and a Big Dye Terminator Cycle Sequencing Kit (Applied Biosystems, Foster City, CA, U.S.A.); the process was performed by GenoScreen (http://www.genoscreen.fr/). In addition, we genotyped each worker at eight microsatellite loci (initially developed for other species: Galarza et al., 2009; Butler, Siletti, Oxley, & Kronauer, 2014). We used multiplex PCRs (described in the Appendix and Table A2).

Nestmate Recognition Bioassays

Behavioural trials were carried out in tandem with the CHC extractions. We employed 79 of the 198 colony fragments used for the CHC extractions; they were chosen from among the largest queenright fragments (>200 workers). In each trial, we placed two ants from different colony fragments in a circular plastic arena (8 cm in dimeter and 5 cm high). For 2 min after the first contact between the ants, we monitored the occurrence of additional contact and aggressive behaviour. We considered that an ant was displaying aggression when it pulled on the other ant's appendages and/or bit the other ant. Trials were given a score of 0 or 1: a 0 was assigned if no aggression was observed, and a 1 was assigned if there was at least one display of aggression. Ant colony identity was not known by the person observing the trial. Ants came either from two colonies within the same population (238 trials) or from two colonies from different populations (430 trials). All interpopulational combinations were tested. The ants were not immediately returned to their nests following the trials so that they would not accidently be used in several tests.

Ethical Note

We adhered to ASAB/ABS's Guidelines for the Use of Animals in Research. All the experiments complied with Spanish laws on animal experimentation. We limited our number of study colonies and replicates as much as possible while still maintaining statistical power. All the ants were treated with care. They were euthanized by freezing prior to CHC extraction. During the behavioural trials (nestmate recognition bioassays), agonistic interactions between ants were not harmful. Ants were kept alive after the trials and were returned to their nests at the end of the experiment.

Data Analysis

The areas of all the CHC peaks that appeared on the GC–MS chromatograms were measured and compared with the area of the internal standard to estimate size-corrected CHC quantities (ng/ant). We performed nonmetric multidimensional scaling (NMDS) analysis using the relative abundances of CHCs. This multivariate approach was carried out using the Bray–Curtis dissimilarity index in the vegan package (Oksanen et al., 2016) for *R* (R Development Core Team, 2015). It allowed us to identify visual differences in CHC profiles between populations. The significance of the observed differences was tested statistically using a randomization test (9999 permutations). Two Pearson correlation tests were performed to examine the relationship between elevation and both the relative abundance of *n*-alkanes and the relative abundance of methyl-branched alkanes.

We then used a Mantel test (9999 permutations) to examine the correlations between matrices of horizontal and vertical distances between populations and chemical dissimilarity between populations.

Finally, we used general linear models (GLMs; Gaussian distribution) to test whether total absolute amounts of *n*-alkanes and methyl-branched alkanes (log-transformed to meet model assumptions) varied with elevation. The mean tibia length of workers from which the CHCs had been extracted was included as the first term in both models.

All the COI sequences were corrected, aligned and analysed using Geneious v. 8.0.3 (http://www.geneious.com, Kearse et al., 2012) and the MAFFT plugin (Katoh, Misawa, Kuma, & Miyata, 2002); the auto option was employed, and the default settings for the other parameters were used. Values were missing for seven samples, which were excluded from subsequent analyses (total: 228 sequences). The pegas package (Paradis, 2010) was used to retrieve haplotypes and create a haplotype network. Haplotype diversity (h) was calculated by hand using Nei's (1987) formula: $h = N\,(1-\sum x_i^2)/(N-1)$, where N is the total number of samples in a population and x_i is the frequency of a given haplotype in that population. Neutrality tests (Tajimas' D; Tajima, 1989) were performed online (http://wwwabi.snv.jussieu.fr/achaz/neutralitytest.html). Each observed value was compared to a

theoretical value generated from 10^5 replicates of the data set without recombination.

To analyse the microsatellite data, we determined allele size and carried out binning using the microsatellite plugin for Geneious. We checked for null alleles and scoring errors at each locus using MicroChecker (Van Oosterhout, Hutchinson, Wills, & Shipley, 2004). Pairwise linkage disequilibrium was tested using GENEPOP ON THE WEB (Raymond & Rousset, 1995; Rousset, 2008). Mean allelic diversity (number of alleles) as well as observed and expected heterozygosity (H_{exp} and H_{obs}, respectively) were determined for each population using the PopGenReport package (Adamack & Gruber, 2014). We used the adegenet package (Jombart, Devillard, & Balloux, 2010) to calculate Nei's (1973) Fst (fixation index) which characterizes the degree of isolation between populations. The significance of the pairwise Fst values was assessed (999 permutations). In addition, we conducted a discriminant analysis of principal components (DAPC) to visualize population differentiation and evaluate the assignment of colonies to each population. DAPC is a robust method for identifying genetic clusters without having to meet Hardy–Weinberg assumptions; it is computationally faster than Bayesian methods. Finally, we employed a Mantel test (999 permutations) to test the relationship between genetic distance (measured as Fst/[1-Fst]) and both elevational and horizontal distances.

The results of the nestmate recognition bioassays were analysed using generalized linear models (glmer), which were carried out with the lme4 package (Bates, Mächler, Bolker, & Walker, 2015). First, we compared the level of between-colony aggression among populations using a glmer model in which the response variable was binomial (presence or absence of aggression). The identity of each colony's population of origin was included as an explanatory variable, and colony identity was a random factor. The significance of the effect of population identity was quantified via model comparison. We also calculated the mean level of aggression between each population pair and compared the resulting matrix of aggression with the matrices of elevational and vertical distances between populations using a Mantel test (999 permutations).

RESULTS

Cuticular Hydrocarbon Analysis

We identified 14 *n*-alkanes and methyl-branched alkanes that occur on the cuticle of *A. iberica* (Table 1). We did not observe any dimethyl alkanes or alkenes. The most abundant compounds had chains of 27 and 29 carbons. Despite pronounced quantitative variation within and between populations, the NMDS analysis (Fig. 1a) tended to distinguish the higher-elevation populations (Z1700 and Z2000) from the lower-elevation ones (Z100–Z1300). The randomization test confirmed that there were significant differences between populations ($R^2 = 0.522$, $P < 0.0001$). Chemical dissimilarity between populations increased significantly with horizontal and vertical distance (Mantel test: $R^2 = 0.67$, $P = 0.002$ and $R^2 = 0.69$, $P = 0.001$, respectively). Horizontal and vertical distance were highly correlated with each other (Mantel test: $R^2 = 0.688$, $P < 0.001$). The relative abundance of methyl-branched alkanes was positively correlated with elevation ($R^2 = 0.816$, $P < 0.001$), while the relative abundance of *n*-alkanes was negatively correlated with elevation (Fig. 1c).

We also analysed variation in the total absolute amounts of *n*-alkanes and methyl-branched alkanes as a function of worker size and elevation. Larger workers had significantly greater quantities of *n*-alkanes (analysis of deviance: $F_{1,\ 196} = 7.47$, $P = 0.007$) but not of methyl-branched alkanes (analysis of deviance: $F_{1,\ 196} = 0.97$, $P = 0.324$). Once the effect of worker size had been removed, the quantity of *n*-alkanes per ant decreased significantly with elevation (Fig. 1b; analysis of deviance: $F_{1,\ 195} = 113.94$, $P < 0.0001$). This pattern was largely explained by the lower C27 levels in higher-elevation populations (analysis of deviance: $F_{1,\ 195} = 344.58$, $P < 0.0001$). In contrast, the total amount of methyl-branched alkanes, of which 3-MC27 was a major contributor, did not change with elevation (Fig. 1d; analysis of deviance: $F_{1,\ 195} = 0.336$, $P = 0.563$). However, the relative abundances of several methyl-branched CHCs did vary with elevation: levels of 3-MC25, 8-MC26 and 4-MC28 decreased significantly with elevation (analysis of deviance: $F_{1,\ 167} = 93.33$, $P < 0.0001$, $F_{1,\ 190} = 249.96$, $P < 0.0001$, $F_{1,\ 183} = 6.77$, $P < 0.01$, respectively), while levels of 11-MC29 and 3-MC29 increased significantly with elevation (analysis of deviance: $F_{1,\ 195} = 17.41$, $P < 0.0001$, $F_{1,\ 195} = 44.81$, $P < 0.0001$, respectively).

Population Genetics

A total of 38 haplotypes and 119 segregating sites were recovered from the 228 sequences (Fig. 2a). Each haplotype was found in a single population. Haplotype diversity was greatest at intermediate elevations (Z600 and Z1000) and decreased at higher

Table 1
Aphaenogaster iberica cuticular CHC composition

CHC	Z100	Z150	Z300	Z600	Z1000	Z1300	Z1700	Z2000
Linear alkanes								
C26	1.7±1.8	4.0±3.0	1.1±1.1	1.1±1.5	2.1±2.3	2.1±1.9	0.8±0.9	1.1±1.0
C27	165.2±86.8	95.4±35.7	82.7±36.9	65.3±45.2	78.0±40.4	49.5±27.1	17.0±13.0	7.3±5.4
C28	13.0±10.8	11.0±7.4	10.7±11.2	7.0±4.8	8.1±4.4	11.6±11.7	8.3±6.1	8.9±3.8
C29	10.3±7.3	3.6±3.3	8.5±4.5	5.6±3.0	7.3±7.8	6.5±5.6	8.1±5.8	16.1±25.7
C30	10.8±3.1	11.5±4.0	9.1±3.7	10.4±3.9	10.5±5.7	15.9±8.7	16.7±6.5	19.7±7.0
Total *n*-alkanes	201.0±97.5	125.4±42.2	112.0±42.8	89.4±53.2	105.9±49.2	85.6±40.7	50.9±22.3	53.1±27.1
Methyl-branched alkanes								
3MC25	2.8±2.2	11.7±8.8	3.2±4.1	1.8±2.4	3.6±5.6	2.7±3.6	0.6±0.6	0.3±0.3
11MC29	19.7±18.8	22.4±12.8	55.3±32.2	46.5±34.1	48.1±25.0	52.7±42.9	48.8±30.2	49.2±22.1
10MC28	7.3±9.6	5.3±4.5	7.9±7.8	2.6±1.6	3.2±4.1	6.6±6.2	5.2±5.8	5.9±5.1
8MC26	9.6±5.6	10.1±6.3	6.2±6.4	4.5±4.6	4.8±4.6	3.9±2.6	1.5±1.8	0.4±0.3
4MC26	1.4±1.8	3.1±2.5	2.1±2.5	0.8±0.9	2.4±4.8	2.6±3.8	1.2±1.2	1.4±1.5
3MC27	110.4±56.5	79.2±23.1	73.2±36.5	70.6±31.3	109.0±48.0	94.5±50.5	62.6±36.4	84.8±46.9
13MC27	25.4±18.9	23.7±12.1	22.0±23.4	14.0±11.1	24.9±26.0	26.1±21.4	21.7±13.1	31.2±49.4
4MC28	3.7±3.8	3.9±3.2	3.4±3.3	1.5±1.3	4.3±6.2	3.4±3.6	1.5±1.4	1.7±1.2
3MC29	4.8±2.1	6.0±1.3	5.4±2.2	5.3±2.3	7.3±2.3	6.7±2.6	7.4±2.7	9.9±3.2
Total methyl-branched alkanes	185.2±89.6	165.4±61.8	178.8±78.6	147.6±75.4	207.7±83.1	199.1±111.4	150.6±63.6	184.7±73.5

Mean and SD of the absolute amounts of CHCs corrected by size (ng per ant) for the eight *Aphaenogaster iberica* study populations, which occurred across an elevational gradient (Z100: 100 m above sea level (asl); Z150: 150 m asl; Z300: 300 m asl; Z600: 600 m asl; Z1000: 1000 m asl; Z1300: 1300 m asl; Z1700: 1700 m asl; Z2000: 2000 m asl).

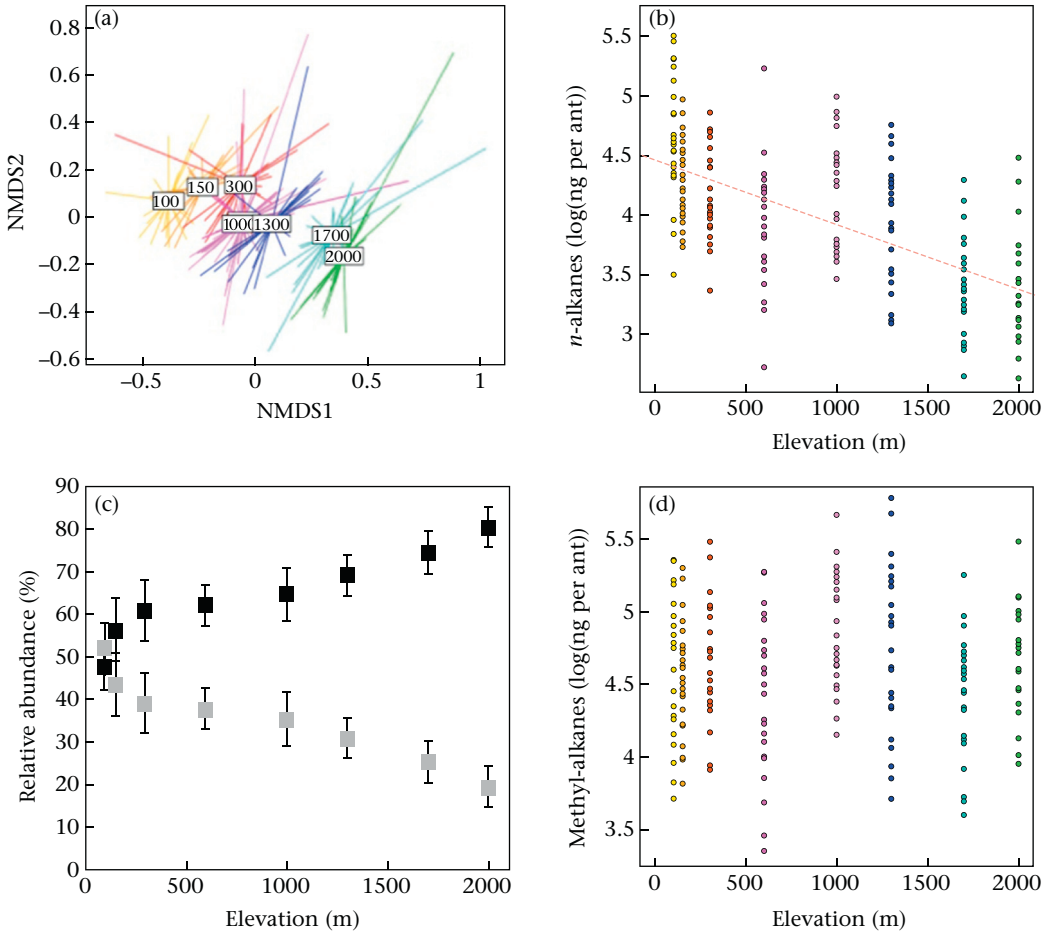

Figure 1. Analysis of variation in *Aphaenogaster iberica* CHC levels across the elevational gradient examined in this study. (a) Profiles based on the relative abundances of CHCs projected along the first NMDS ordination axis. (b) Variation in the absolute quantities of *n*-alkanes with elevation. (c) Mean and SD of the relative abundances of *n*-alkanes (grey squares) and methyl-branched alkanes (black squares) for each study population. (d) Variation in the absolute quantities of methyl-branched alkanes with elevation.

elevations (Table 2). The haplotype network (Fig. 2b) analysis showed that neighbouring populations had more similar haplotypes than did more distant ones. The only exception was Z1000, which contained two haplogroups; one was related to the haplotypes of Z300 and Z600 and the other to the haplotypes of Z1300 and Z1700. However, there were no signs of local spatial segregation between these haplogroups in Z1000 (Fig. 2a). The Tajima's *D* analysis indicated that there was a significant departure from neutrality in Z100 and Z1300 and a marginally significant departure from neutrality in Z600 (Table 2). However, after examining the data set, we found that haplotype II in Z100 had accumulated 45% of all the segregating sites. This sample greatly influenced the analysis, and, after its removal, Tajima's *D* became nonsignificant in Z100. However, in Z1300, the result for Tajima's *D* was consistent with the underrepresentation of a rare haplotype.

There were 2–45 alleles at each of the eight microsatellite loci. Only two of the 28 linkage disequilibrium tests yielded significant results (Table A3). There was a significant deficit of heterozygotes in Z1000 (Table 2). The global Fst value (calculated over all the populations) was low (Fst = 0.032) but highly significant ($P = 0.002$). All but seven pairwise Fst comparisons (out of 28) were significant, which indicates that there was generally a high level of genetic differentiation, except between neighbouring mid-elevation populations (Table 3). The DAPC results showed that Z1700 and Z2000 were more genetically differentiated than were the other populations (Fig. 3a). Assignment probabilities were also better for the high-elevation populations (Z1700 and Z2000) than for the low-elevation populations, which denotes the greater genetic differentiation between the former (Fig. 3b). We also found evidence of isolation by distance between populations that was related to elevation but not to horizontal distance. Hence, the genetic distance between populations, as estimated with Fst/(1−Fst), was significantly correlated with elevation (Mantel test: $R^2 = 0.561$, $P = 0.004$; Fig. 3c) but not with horizontal distance (Mantel test: $R^2 = 0.137$, $P = 0.205$; Fig. 3d).

Nestmate Recognition

The mean level of aggression among workers from different colonies within the same population was relatively low and did not differ significantly between populations (model comparison: with versus without population identity as a main effect: difference in the Akaike information criterion, AIC: 13.27, $\chi^2_8 = 0.728$, $P = 0.998$). Therefore, it appears that levels of aggression between non-nestmates within a given population did not differ between populations.

The level of aggression between colonies from different populations increased significantly with the horizontal and elevational distance between populations (Mantel test: $R^2 = 0.457$, $P = 0.019$ and $R^2 = 0.642$, $P = 0.002$, respectively; Fig. 4). It also increased significantly with genetic distance and CHC dissimilarity between populations (Mantel test: $R^2 = 0.488$, $P = 0.046$ and $R^2 = 0.589$,

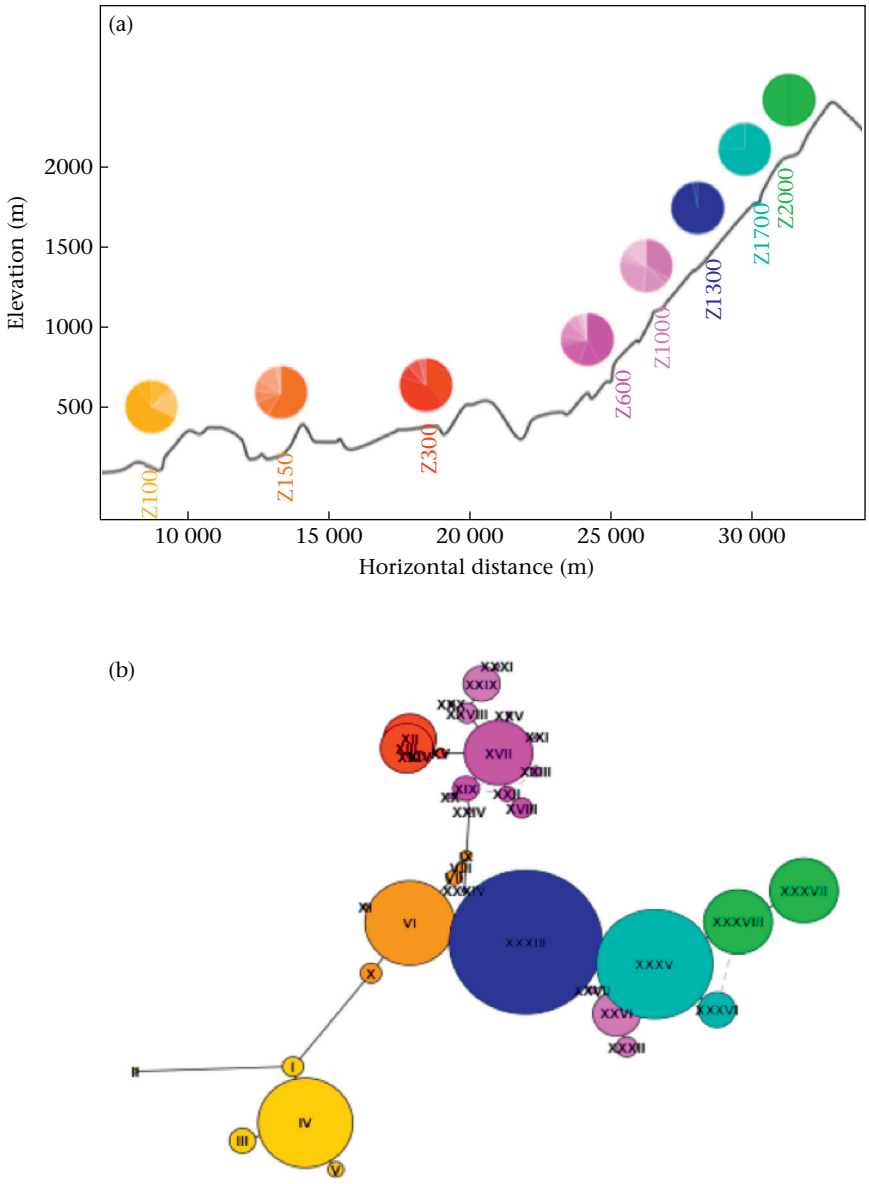

Figure 2. Haplotype diversity along the elevational gradient. (a) The pie charts indicate the number of haplotypes per population. (b) The network shows the relationship between haplotypes. The colours refer to the populations in which the haplotypes were found. Circle size represents haplotype frequency.

Table 2
Mitochondrial and microsatellite genetic analyses for the eight *Aphaenogaster iberica* study populations

Populations	Mitochondrial DNA					Microsatellite DNA				
	N	*h*	*S*	D_{obs}	$P\,(D_{obs} > D_{theo})$	*N*	NA	H_{exp}	H_{obs}	$P\,(H_{obs} \neq H_{exp})$
Z100	31	0.63	57	-2.58	<0.001	31	7.75	0.656	0.659	0.099
	30	*0.60*	*4*	*-0.02*	*0.542*					
Z150	29	0.64	13	0.30	0.676	30	7.09	0.619	0.630	0.711
Z300	25	0.69	7	0.17	0.624	25	7.13	0.654	0.657	0.998
Z600	30	0.79	12	-1.49	0.050	30	7.56	0.645	0.597	0.075
Z1000	28	0.80	27	3.26	1.000	32	6.66	0.646	0.605	0.014
Z1300	30	0.07	1	-1.14	<0.001	30	7.60	0.642	0.629	0.106
Z1700	29	0.38	1	0.77	0.698	30	7.66	0.649	0.641	0.931
Z2000	26	0.52	1	2.11	0.995	27	6.88	0.647	0.652	0.192

For the mitochondrial data, the columns indicate sample size (*N*), haplotype diversity (*h*), number of segregating sites (*S*), Tajima's *D* (D_{obs}) and Tajima's *D* theoretical value (D_{theo}) generated from 10^5 replicates of the data set and the associated *P* values. Note that for Z100, the first row includes haplotype II with 57 segregation sites. The second row in italics does not include this haplotype. For the microsatellite DNA, the columns indicate sample size (*N*), allele diversity (NA), expected heterozygosity (H_{exp}), observed heterozygosity (H_{obs}) and the associated *P* values.

Table 3
Pairwise differentiation test for *Aphaenogaster iberica* populations

	Z100	Z150	Z300	Z600	Z1000	Z1300	Z1700	Z2000
Z100	–	1.000	1.000	0.184	0.008	0.008	0.008	0.008
Z150	0.011	–	0.016	0.008	0.008	0.008	0.008	0.008
Z300	0.011	0.022	–	1.000	0.016	0.008	0.008	0.008
Z600	0.014	0.023	0.012	–	1.000	1.000	0.008	0.008
Z1000	0.025	0.036	0.02	0.011	–	1.000	0.008	0.008
Z1300	0.019	0.028	0.019	0.01	0.009	–	0.008	0.008
Z1700	0.022	0.028	0.034	0.026	0.028	0.021	–	0.008
Z2000	0.033	0.035	0.045	0.042	0.052	0.04	0.029	–

Pairwise values of Nei's *F*st for the eight *Aphaenogaster iberica* study populations (below the diagonal) and the associated Bonferroni-corrected *P* values (above the diagonal).

$P = 0.002$, respectively; Fig. 4). Finally, the correlation between the level of aggression and CHC dissimilarity remained significant even after accounting for the correlation between genetic distance and aggression (partial Mantel test: $R^2 = 0.545$, $P = 0.006$).

DISCUSSION

In southern Spain, the ant *A. iberica* is distributed over a large elevational gradient with very contrasted environmental conditions. Low-elevation populations experience a hot Mediterranean climate that limits colony activity during the warmest hours of the summer. In contrast, high-elevation populations experience short summers and are exposed to cold and humid conditions; they need to be active even at low temperatures and high relative humidity levels to build up sufficient stores of energy. The present study shows that these climatic conditions are likely to be correlated with major differences in CHC profiles.

One of the principal functions of CHCs is to protect insect bodies against desiccation. In Mediterranean habitats, mechanisms of insect resistance to desiccation and to high temperatures are intimately linked. Because *n*-alkanes are more stable at high temperatures than are methyl-branched alkanes, they also provide more effective protection against dry conditions. As elevation increases, temperature decreases, and the need for large amounts of *n*-alkanes is likely to become less crucial.

The greatest difference we observed was in *n*-alkanes, whose total absolute quantity decreased with increasing elevation. There was also variation in the levels of several methyl-branched alkanes, even though the total quantity of methyl-branched alkanes was not significantly different between populations. We also found that populations, particularly those at higher elevations, were significantly genetically isolated. This may promote the evolution of local adaptations, although the operation of other evolutionary processes cannot be excluded. Finally, CHC dissimilarity between populations was positively correlated with aggression; however,

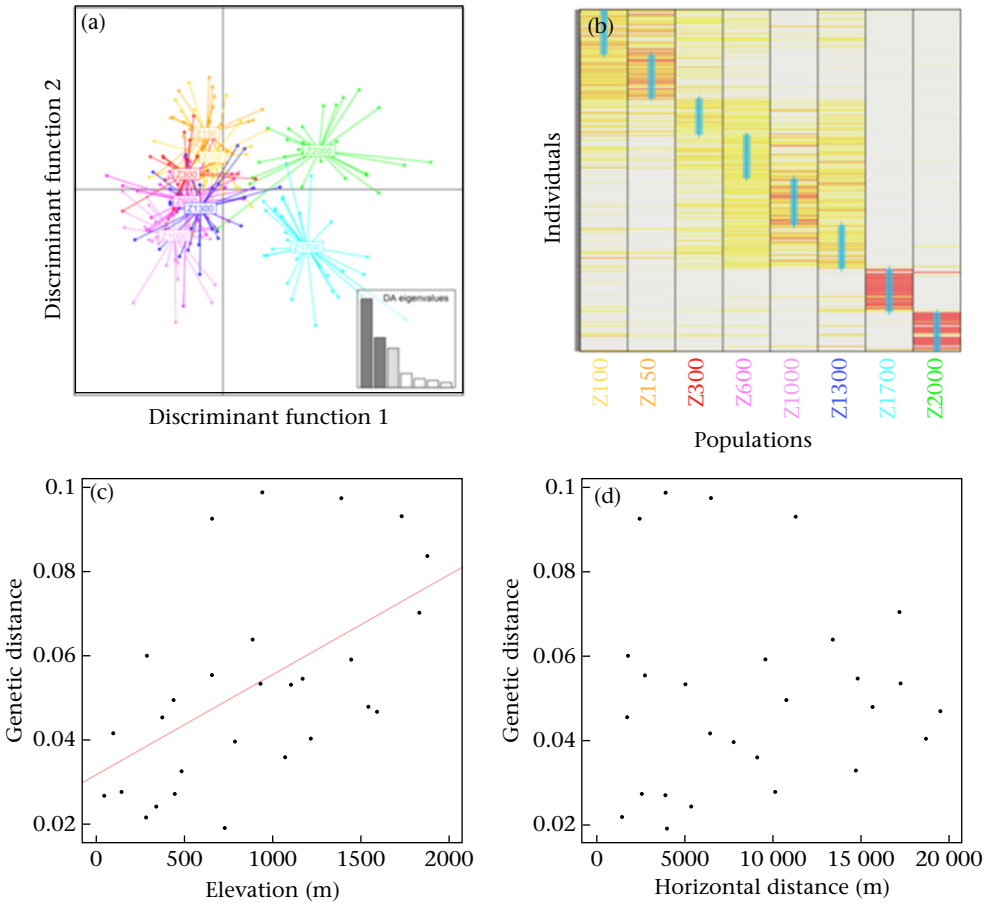

Figure 3. Results of the microsatellite analyses for the eight *Aphaenogaster iberica* study populations. (a) Discriminant analysis showing the differentiation between Z1700 and Z2000 and the other populations found at lower elevations. The inset show the relative magnitude of eigenvalues retained for the DAPC analysis . The first two DA eigenvalues are highlighted in dark grey and correspond to the horizontal and vertical axes, respectively. (b) Probability of individuals being assigned to each population. High probabilities are indicated by colours, whereas low probabilities are indicated in grey. The blue crosses indicate the real origin of the individuals. Note how the assignment probability is much higher for Z1700 and Z2000. (c) Relationship between the genetic distance and the elevational distance of different populations. (d) Relationship between the genetic distance and horizontal distance between different populations.

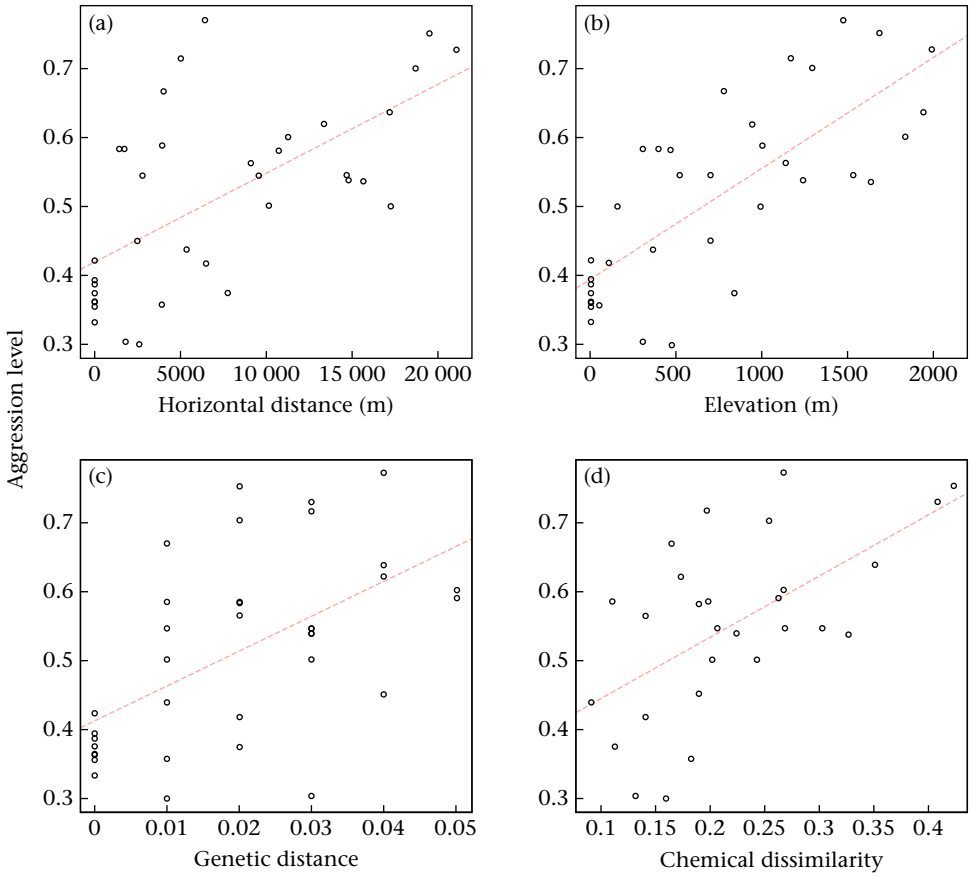

Figure 4. Relationship between the level of aggression and (a) horizontal distance, (b) elevational distance, (c) genetic distance (estimated using Fst/[1-Fst]) and (d) CHC dissimilarity (estimated using the Bray–Curtis index) between colonies. See the Results for further details.

elevational changes in CHCs had no effect on aggression among colonies within populations. These results therefore suggest that, although environmental and genetic constraints may affect the ants' CHC profiles, they do not necessarily lead to pronounced differences in CHCs between competing colonies.

Other studies have found that insect CHCs vary along climatic gradients. For example, the CHC profiles of two *Drosophila* species were shown to vary along the coast of eastern Australia (Frentiu & Chenoweth, 2010). A similar result was obtained along the eastern coast of the U.S.A. (Rajpurohit et al., 2017). In the latter study, the researchers found that flies in warmer locations had heavier compounds, which fits with the hypothesis that heavier compounds are more thermostable than lighter ones. In ants, a recent comparative study showed that, across species, the ratio of dimethyl alkanes to alkenes was correlated with rainfall level (Menzel et al., 2017, 2018). However, a limitation of these studies is that they generally examine relative abundances of CHCs; desiccation resistance is more likely to be determined by absolute quantities. We adopted a more quantitative approach here, and we discovered that absolute amounts of *n*-alkanes decreased significantly with increasing elevation. More importantly, this relationship remained significant even after controlling for the confounding effect of worker size. Worker body size tends to increase with elevation (Villalta et al., 2019), and larger workers logically bear greater amounts of CHCs.

At least two nonmutually exclusive evolutionary mechanisms could explain CHC differences along the elevational gradient we studied. First, ants may adjust *n*-alkane synthesis or degradation to environmental conditions through phenotypic plasticity. This phenomenon has been seen in several ant species that were able to acclimate to warmer conditions in a matter of weeks by producing relatively higher levels of *n*-alkanes and relatively lower levels of methyl-branched alkanes (Sprenger et al., 2018). In our study, we were not able to sample a colony's CHCs immediately after its collection in the field. Otherwise, we would have been able to characterize the degree of chemical drift that took place after colonies had spent 8 months experiencing the same laboratory conditions. However, we can assume that this time period was long enough to reduce short-term environment-induced differences between populations. Thus, the CHC differences that we observed here were more likely to be genetically and/or epigenetically modulated.

Second, rapid evolution in CHC profiles has occurred in *Drosophila* flies in response to new environmental conditions (Rajpurohit et al., 2017). In nature, evolution may lead to local adaptations if populations experience contrasting selection pressures, which is the case for *A. iberica*. In addition, populations must be sufficiently isolated so that gene flow among them does not prevent the fixation of different alleles. Even though populations of *A. iberica* were separated by a few kilometres, both the mitochondrial and microsatellite markers indicated that they were clearly genetically distinct. Gene flow is low even among neighbouring populations, a fact that is partly linked to this species' mode of colony founding. Since they disperse by foot, females travel no more than a few metres during each dispersal event. Nest relocations are frequent, which limits the degree of isolation by distance within populations. However, they are unlikely to promote gene exchange among populations (Galarza et al., 2012), which

helps explain why each haplotype was only present in a single population. The significant Tajima's *D* in Z1300 pointed to the existence of rare alleles, which could be due to a recent bottleneck. More generally, the negative correlation between haplotype diversity and elevation may suggest that some areas were recently colonized and/or that populations have declined in size. The wildfire that occurred in 2005 in higher elevation areas may have had an impact on *A. iberica* populations found above 1300 m. Moreover, the extreme environmental conditions experienced by these populations may constrain reproduction, colonization and diversification dynamics.

The microsatellite analysis also indicated that genetic distance increased with increasing elevation and that the two highest populations were more isolated than the others. This result suggests that any gene flow taking place via the dispersal of winged males is not enough to prevent the genetic differentiation of populations. A similar result was seen in the fission-performing ant *Cataglyphis cursor* (Clémencet, Viginier, & Doums, 2005). Moreover, in mountainous habitats, male dispersal may be restricted by strong wind currents, which can prevent males from dispersing to higher elevations (Jowers et al., 2013). Finally, differences in thermal conditions between higher and lower elevations may lead to differences in the timing of production of male and female reproductives between populations (Woodward et al., 2010). Even if males from lower elevations are able to reach higher ones, they may arrive too early in the season or be unsuited to local conditions; consequently, they may be less likely than resident males to mate with resident queens.

The level of aggression between colonies from different populations increased with elevational, horizontal and genetic distance as well as with CHC dissimilarity. This finding lends support to the graded model of nestmate recognition, in which a behavioural response is proportional to signal dissimilarity (Ichinose, Cerda, Christidès, & Lenoir, 2005; Sturgis & Gordon, 2012). At first glance, this model may seem counterintuitive because, under natural conditions, colonies should be able to fully recognize and exclude sympatric competitors in a more binary way (Boulay et al., 2010, 2007). Aggression may be constrained by the diversity of genetic and/or environmental recognition cues among sympatric colonies (Beye, Neumann, Chapuisat, Pamilo, & Moritz, 1998; but see ; Martin, Vitikainen, Drijfhout, & Jackson, 2012). One possible explanation is that CHC variation resulting from differences in *n*-alkane biosynthesis could have affected the biosynthetic pathways of several methyl-branched alkanes, which could have promoted a continuous change in methyl-branched alkane blends along the elevational gradient we studied. Although *n*-alkanes are involved in pheromonal communication in some ant species (Van Oystaeyen et al., 2014), several studies have shown that they convey less precise information about colony identity than do methyl-branched alkanes, namely because of the latter's greater structural variability (Guerrieri et al., 2009; Martin & Drijfhout, 2009). In our study, the decline in *n*-alkane levels with increasing elevation probably acted to limit the relative abundance of methyl-branched alkanes in the *A. iberica* populations that we studied. This environmental constraint explained, at least in part, the population level differences in colony CHC profiles and thus probably contributed to increased aggression among colonies from different populations.

Over the next century, climate warming is expected to have particularly strong effects in mountainous regions. Although this study is the first step in a longer line of research, our results reveal that climate change may have an unanticipated impact on insect behaviour due to the pleiotropy of major traits such as CHC profiles, which are involved in both communication and resistance to abiotic conditions.

Acknowledgments

We thank Alain Lenoir for his comments on the manuscript, Jessica Pearce for her assistance with the English language editing, Abraham Hefetz for CHC identification and Séverine Devers and Cristela Sanchez for their help with CHC and DNA extractions. This project was supported by the following grants: PICS #24698 from CNRS to R.B.; P12-RNM-2705 from the Andalusian Regional Government (Junta de Andalucía Projects of Excellence 2012; Consejería de Innovación, Ciencia y Empleo) to I.V., R.B. and X.C.; project CGL2015-65807-P from the Spanish Ministry of Economy and Competitiveness and FEDER to X.C., R.B. and I.V.

Supplementary data

Supplementary data associated with this article can be found, in the online version, at https://doi.org/10.1016/j.anbehav.2019.11.008.

References

Adamack, A. T., & Gruber, B. (2014). PopGenReport: Simplifying basic population genetic analyses in R. *Methods in Ecology and Evolution, 5*(4), 384–387. https://doi.org/10.1111/2041-210X.12158.

Alcántara, J. M., Rey, P. J., Manzaneda, A. J., Boulay, R., Ramírez, J. M., & Fedriani, J. M. (2007). Geographic variation in the adaptive landscape for seed size at dispersal in the myrmecochorous *Helleborus foetidus*. *Evolutionary Ecology, 21*, 411–430. https://doi.org/10.1007/s10682-006-9110-3.

Bates, D., Mächler, M., Bolker, B. M., & Walker, S. C. (2015). Fitting linear mixed-effects models using lme4. *Journal of Statistical Software, 67*(1), 1–48. https://doi.org/10.18637/jss.v067.i01.

Beye, M., Neumann, P., Chapuisat, M., Pamilo, P., & Moritz, R. F. A. (1998). Nestmate recognition and the genetic relatedness of nests in the ant *Formica pratensis*. *Behavioral Ecology and Sociobiology, 43*(1), 67–72. https://doi.org/10.1007/s002650050467.

Blomquist, G. J., & Bagnères, A. (Eds.). (2010). *Insect hydrocarbons biology, biochemistry, and chemical ecology*. Cambridge, U.K.: Cambridge University Press. https://doi.org/10.1017/CBO9780511711909.

Bonavita-Cougourdan, A., Clément, J. L., & Lange, C. (1987). Nestmate recognition: The role of cuticular hydrocarbons in the ant, *Camponotus vagus* Scop. *Journal of Entomological Science, 22*(1), 1–10. https://doi.org/10.18474/0749-8004-22.1.1.

Boulay, R., Cerdá, X., Simon, T., Roldan, M., & Hefetz, A. (2007). Intraspecific competition in the ant *Camponotus cruentatus*: Should we expect the "dear enemy" effect? *Animal Behaviour, 74*(4), 985–993. https://doi.org/10.1016/j.anbehav.2007.02.013.

Boulay, R., Galarza, J. A., Chéron, B., Hefetz, A., Lenoir, A., Van Oudenhove, L., et al. (2010). Intraspecific competition affects population size and resource allocation in an ant dispersing by colony fission. *Ecology, 91*, 3312–3321. https://doi.org/10.1890/09-1520.1.

Boulay, R., Hefetz, A., Soroker, V., & Lenoir, A. (2000). *Camponotus fellah* colony integration: Worker individuality necessitates frequent hydrocarbon exchanges. *Animal Behaviour, 59*, 1127–1133. https://doi.org/10.1006/anbe.2000.1408.

Boulay, R., Katzav-Gozansky, T., Hefetz, A., & Lenoir, A. (2004). Odour convergence and tolerance between nestmates through trophallaxis and grooming in the ant *Camponotus fellah* (Dalla Torre). *Insectes Sociaux, 51*, 55–61. https://doi.org/10.1007/s00040-003-0706-0.

Butler, I. A., Siletti, K., Oxley, P. R., & Kronauer, D. J. C. (2014). Conserved microsatellites in ants enable population genetic and colony pedigree studies across a wide range of species. *PLoS One, 9*(9), e107334. https://doi.org/10.1371/journal.pone.0107334.

Clémencet, J., Viginier, B., & Doums, C. (2005). Hierarchical analysis of population genetic structure in the monogynous ant *Cataglyphis cursor* using microsatellite and mitochondrial DNA markers. *Molecular Ecology, 14*, 3735–3744. https://doi.org/10.1111/j.1365-294X.2005.02706.x.

Crozier, R. H., & Dix, M. W. (1979). Analysis of two genetic models for innate components of colony odour in social hymenoptera. *Behavioral Ecology and Sociobiology, 4*, 217–224.

Dahbi, A., Hefetz, A., Cerdá, X., & Lenoir, A. (1999). Trophallaxis mediates uniformity of colony odor in *Cataglyphis iberica* ants (Hymenoptera, Formicidae). *Journal of Insect Behavior, 12*(4), 559–567. https://doi.org/10.1023/A:1020975009450.

Dudaniec, R. Y., Yong, C. J., Lancaster, L. T., Svensson, E. I., & Hansson, B. (2018). Signatures of local adaptation along environmental gradients in a range-expanding damselfly (*Ischnura elegans*). *Molecular Ecology, 27*(11), 2576–2593. https://doi.org/10.1111/mec.14709.

D'Ettorre, P., & Lenoir, A. (2010). Nestmate recognition. In L. Lach, C. L. Parr, & K. Abbott (Eds.), *Ant ecology* (pp. 194–209). Oxford, U.K: Oxford University Press. https://doi.org/10.1093/acprof.

Frentiu, F. D., & Chenoweth, S. F. (2010). Clines in cuticular hydrocarbons in two drosophila species with independent population histories. *Evolution, 64*(6), 1784–1794. https://doi.org/10.1111/j.1558-5646.2009.00936.x.

Galarza, J. A., Boulay, R., Cerda, X., Doums, C., Federici, P., Magalon, H., et al. (2009). Development of single sequence repeat markers for the ant *Aphaenogaster senilis* and cross-species amplification in *A. iberica, A . gibbosa, A. subterranea* and *Messor maroccanus*. *Conservation Genetics, 10*(3), 519–521. https://doi.org/10.1007/s10592-008-9554-9.

Galarza, J. A., Jovani, R., Cerdá, X., Rico, C., Barroso, A., & Boulay, R. (2012). Frequent colony relocations do not result in effective dispersal in the gypsy ant *Aphaenogaster senilis*. *Oikos, 121*(4), 605–613. https://doi.org/10.1111/j.1600-0706.2011.19859.x.

Gibbs, A. (1995). Physical properties of insect cuticular hydrocarbons: Model mixtures and lipid interactions. *Comparative Biochemistry and Physiology B: Biochemistry and Molecular Biology, 112*, 667–672. https://doi.org/10.1016/0305-0491(95)00081-X.

Gibbs, A. G., Louie, A. K., & Ayala, J. A. (1998). Effects of temperature on cuticular lipids and water balance in a desert *Drosophila*: Is thermal acclimation beneficial? *Journal of Experimental Biology, 80*, 71–80.

Gibbs, A., & Pomonis, J. G. (1995). Physical properties of insect cuticular hydrocarbons: The effects of chain length, methyl-branching and unsaturation. *Comparative Biochemistry and Physiology B: Biochemistry & Molecular Biology, 112*(2), 243–249. https://doi.org/10.1016/0305-0491(95)00081-X.

Gibbs, A. G., & Rajpurohit, S. (2010). Cuticular lipids and water balance. In G. J. Blomquist, & A.-G. Bagnères (Eds.), *Insect hydrocarbons: Biology, biochemistry, and chemical ecology* (pp. 100–120). Cambridge, U.K.: Cambridge University Press. https://doi.org/10.1017/CBO9780511711909.007.

Guerrieri, F. J., Nehring, V., Jø rgensen, C. G., Nielsen, J., Galizia, C. G., & D'Ettorre, P. (2009). Ants recognize foes and not friends. *Proceedings of the Royal Society B: Biological Sciences, 276*(1666), 2461–2468. https://doi.org/10.1098/rspb.2008.1860.

Hadley, N. F. (1978). Cuticular permeability of desert tenebrionid beetles: Correlations with epicuticular hydrocarbon composition. *Insect Biochemistry, 8*(1), 17–22. https://doi.org/10.1016/0020-1790(78)90005-7.

Ichinose, K., Cerda, X., Christidès, J.-P., & Lenoir, A. (2005). Detecting nestmate recognition patterns in the fission-performing ant *Aphaenogaster senilis*: A comparison of different indices. *Journal of Insect Behavior, 18*(5), 633–650. https://doi.org/10.1007/s10905-005-7016-5.

Jallon, J. M., & David, J. R. (1987). Variations in cuticular hydrocarbons among the eight species of the *Drosophila melanogaster* subgroup. *Evolution, 41*(2), 294–302. https://doi.org/10.2307/2409139.

Johnson, R. A., & Gibbs, A. G. (2004). Effect of mating stage on water balance , cuticular hydrocarbons and metabolism in the desert harvester ant, *Pogonomyrmex barbatus*. *Journal of Insect Physiology, 50*, 943–953. https://doi.org/10.1016/j.jinsphys.2004.07.006.

Jombart, T., Devillard, S., & Balloux, F. (2010). Discriminant analysis of principal components: A new method for the analysis of genetically structured populations. *BMC Genetics, 11*, 94. https://doi.org/10.1186/1471-2156-11-94.

Jowers, M. J., Leniaud, L., Cerdá, X., Alasaad, S., Caut, S., Amor, F., et al. (2013). Social and population structure in the ant *Cataglyphis emmae*. *PLoS One, 8*(9), e72941. https://doi.org/10.1371/journal.pone.0072941.

Katoh, K., Misawa, K., Kuma, K., & Miyata, T. (2002). MAFFT: A novel method for rapid multiple sequence alignment based on fast Fourier transform. *Nucleic Acids Research, 30*(14), 3059–3066. https://doi.org/10.1093/nar/gkf436.

Kawecki, T. J., & Ebert, D. (2004). Conceptual issues in local adaptation. *Ecology Letters, 7*(12), 1225–1241. https://doi.org/10.1111/j.1461-0248.2004.00684.x.

Kearse, M., Moir, R., Wilson, A., Stones-Havas, S., Cheung, M., Sturrock, S., et al. (2012). Geneious Basic: An integrated and extendable desktop software platform for the organization and analysis of sequence data. *Bioinformatics, 28*(12), 1647–1649. https://doi.org/10.1093/bioinformatics/bts199.

Lahav, S., Soroker, V., Hefetz, A., & Vander Meer, R. K. (1999). Direct behavioral evidence for hydrocarbons as ant recognition discriminators. *Naturwissenschaften, 86*(5), 246–249. https://doi.org/10.1007/s001140050609.

Lenoir, A., Fresneau, D., Errard, C., & Hefetz, A. (1999). Individuality and colonial identity in ants: The emergence of the social representation concept. In C. Detrain, J. Deneubourg, & J. Pasteels (Eds.), *Information processing in social insects* (pp. 219–237). Bâle, Switzerland: Birkhäuser Verlag. https://doi.org/10.1007/978-3-0348-8739-7_12.

Liang, D., & Silverman, J. (2000). "You are what you eat": Diet modifies cuticular hydrocarbons and nestmate recognition in the Argentine ant, *Linepithema humile*. *Naturwissenschaften, 87*(9), 412–416. https://doi.org/10.1007/s001140050752.

Martin, S., & Drijfhout, F. (2009). A review of ant cuticular hydrocarbons. *Journal of Chemical Ecology, 35*, 1151–1161. https://doi.org/10.1007/s10886-009-9695-4.

Martin, S. J., Vitikainen, E., Drijfhout, F. P., & Jackson, D. (2012). Conspecific ant aggression is correlated with chemical distance, but not with genetic or spatial distance. *Behavior Genetics, 42*, 323–331. https://doi.org/10.1007/s10519-011-9503-0.

Martin, S. J., Vitikainen, E., Helanterä, H., & Drijfhout, F. P. (2008). Chemical basis of nest-mate discrimination in the ant *Formica exsecta*. *Proceedings of the Royal Society B: Biological Sciences, 275*(1640), 1271–1278. https://doi.org/10.1098/rspb.2007.1708.

Martin, S. J., Vitikainen, E., Shemilt, S., Drijfhout, F. P., & Sundström, L. (2013). Sources of variation in cuticular hydrocarbons in the ant *Formica exsecta*. *Journal of Chemical Ecology, 39*(11–12), 1415–1423. https://doi.org/10.1007/s10886-013-0366-0.

Menzel, F., Blaimer, B. B., & Schmitt, T. (2017). How do cuticular hydrocarbons evolve? Physiological constraints and climatic and biotic selection pressures act on a complex functional trait. *Proceedings of the Royal Society B: Biological Sciences, 284*, 20161727. https://doi.org/10.1098/rspb.2016.1727.

Menzel, F., Zumbusch, M., & Feldmeyer, B. (2018). How ants acclimate: Impact of climatic conditions on the cuticular hydrocarbon profile. *Functional Ecology, 32*(3), 657–666. https://doi.org/10.1111/1365-2435.13008.

Morgan, E. D. (2004). Fatty acids and derived compounds. In G. J. Blomquist (Ed.), *Biosynthesis in insects* (pp. 28–56). Cambridge, U.K: Cambridge University Press. https://doi.org/10.1017/CBO9780511711909.007.

Nei, M. (1973). Analysis of gene diversity in subdivided populations. *Proceedings of the National Academy of Sciences, 70*(12), 3321–3323. https://doi.org/10.1073/pnas.70.12.3321.

Nei, M. (1987). *Molecular evolutionary genetics*. NewYork, NY: Columbia University Press.

Nosil, P. (2012). *Ecological speciation*. Oxford, U.K.: Oxford University Press.

Obin, M. S., & Vander Meer, R. K. (1988). Sources of nestmate recognition in the imported fire ant *Solenopsis invicta* Buren (Hymenoptera: Formicidae). *Animal Behaviour, 36*(5), 1361–1370. https://doi.org/10.1016/S0003-3472(88)80205-7.

Oksanen, J., Blanchet, F. G., Kindt, R., Legendre, P., Minchin, P. R., O'Hara, R. B., et al. (2016). *Vegan: community ecology package. R package vegan, vers. 2.2-1*. Retrieved from https://cran.r-project.org/package=vegan.

Paradis, E. (2010). pegas: an R package for population genetics with an integrated modular approach. *Bioinformatics, 26*(3), 419–420. https://doi.org/10.1093/bioinformatics/btp696.

Provost, E. (1991). Nonnestmate kin recognition in the ant *Leptothorax lichtensteini*: Evidence the genetic factors regulate colony recognition. *Behavior Genetics, 21*(2), 151–167. https://doi.org/10.1007/BF01066333.

R Development Core Team. (2015). *R: a language and environment for statistical computing*. Vienna, Austria: R Foundation for Statistical Computing. https://doi.org/10.1038/sj.hdy.6800737.

Rajpurohit, S., Hanus, R., Vrkoslav, V., Behrman, E. L., Bergland, A. O., Petrov, D., et al. (2017). Adaptive dynamics of cuticular hydrocarbons in *Drosophila*. *Journal of Evolutionary Biology, 30*, 66–80. https://doi.org/10.1111/jeb.12988.

Räsänen, K., & Hendry, A. P. (2008). Disentangling interactions between adaptive divergence and gene flow when ecology drives diversification. *Ecology Letters, 11*. https://doi.org/10.1111/j.1461-0248.2008.01176.x.

Raymond, M., & Rousset, F. (1995). GENEPOP (version 1.2): Population genetics software for exact tests and ecumenicism. *Journal of Heredity, 86*(3), 248–249. https://doi.org/10.1093/oxfordjournals.jhered.a111573.

Rouault, J.-D., Capy, P., & Jallon, J. M. (2000). Variations of male cuticular hydrocarbons with geoclimatic variables: An adaptative mechanism in *Drosophila melanogaster*? *Genetica, 110*(2), 117–130. https://doi.org/10.1023/A:1017987220814.

Rourke, B. C. (2000). Geographic and altitudinal variation in water balance and metabolic rate in a California grasshopper, *Melanoplus sanguinipes*. *Journal of Experimental Biology, 203*(17), 2699–2712.

Rousset, F. (2008). Genepop'007: A complete reimplementation of the Genepop software for Windows and Linux. *Molecular Ecology Resources, 8*, 103–106. https://doi.org/10.1111/j.1471-8286.2007.01931.x.

Schneider, C. A., Rasband, W. S., & Eliceiri, K. W. (2012). NIH image to ImageJ: 25 years of image analysis. *Nature Methods, 9*(7), 671–675. https://doi.org/10.1038/nmeth.2089.

Sharma, M., Mitchell, C., Hunt, J., Tregenza, T., & Hosken, D. (2012). The genetics of cuticular hydrocarbon profiles in the fruit fly *Drosophila simulans*. *Journal of Heredity, 103*(2), 230–239. https://doi.org/10.1093/jhered/esr132.

Soroker, V., Vienne, C., & Hefetz, A. (1995). Hydrocarbon dynamics within and between nestmates in *Cataglyphis niger* (hymenoptera: Formicidae). *Journal of Chemical Ecology, 21*(3), 365–378. https://doi.org/10.1007/BF02036724.

Sprenger, P. P., Burkert, L. H., Abou, B., Federle, W., & Menzel, F. (2018). Coping with the climate: Cuticular hydrocarbon acclimation of ants under constant and fluctuating conditions. *Journal of Experimental Biology*. https://doi.org/10.1242/jeb.171488.

Sturgis, S. J., & Gordon, D. M. (2012). Nestmate recognition in ants (hymenoptera: Formicidae): A review. *Myrmecological News, 16*, 101–110.

Tajima, F. (1989). Statistical method for testing the neutral mutation hypothesis by DNA polymorphism. *Genetics, 123*(3), 585–595. http://doi.org/PMC1203831.

Thompson, J. N. (1999). Specific hypotheses on the geographic mosaic of coevolution. *The American Naturalist, 153*(S5), S1–S14. https://doi.org/10.1086/303208.

Toolson, E. C. (1982). Effects of rearing temperature on cuticle permeability and epicuticular lipid composition in *Drosophila pseudoobscura*. *Journal of Experimental Zoology, 222*(3), 249–253. https://doi.org/10.1002/jez.1402220307.

Toolson, E. C., & Hadley, N. F. (1979). Seasonal effects on cuticular permeability and epicuticular lipid composition in *Centruroides sculpturatus* Ewing 1928 (Scorpiones: Buthidae). *Journal of Comparative Physiology, 129*(4), 319–325. https://doi.org/10.1007/BF00686988.

Van Oosterhout, C., Hutchinson, W. F., Wills, D. P. M., & Shipley, P. (2004). MICRO-CHECKER: Software for identifying and correcting genotyping errors in microsatellite data. *Molecular Ecology Notes, 4*(3), 535–538. https://doi.org/10.1111/j.1471-8286.2004.00684.x.

Van Oystaeyen, A., Oliveira, R. C., Holman, L., van Zweden, J. S., Romero, C., Oi, C. A., et al. (2014). Conserved class of queen pheromones stops social insect workers from reproducing. *Science, 343*(6168), 287–290. https://doi.org/10.1126/science.1244899.

Villalta, I., Abril, S., Cerdá, X., & Boulay, R. (2018). Queen control or queen signal in ants: What remains of the controversy 25 Years after Keller and Nonacs' seminal paper? *Journal of Chemical Ecology, 44*, 805–817. https://doi.org/10.1007/s10886-018-0974-9.

Villalta, I., Sánchez-Oms, C., Angulo, E., Molinas-González, C. R., Devers, S., Cerdá, X., et al. (2019). *Does social thermoregulation constrain individual thermotolerance in an ant species?*. Manuscript in preparation.

Wagner, D., Tissot, M., Cuevas, W., & Gordon, D. M. (2000). Harvester ants utilize cuticular hydrocarbons in nestmate recognition. *Journal of Chemical Ecology, 26*(10), 2245–2257. https://doi.org/10.1023/A:1005529224856.

Wagner, D., Tissot, M., & Gordon, D. (2001). Task-related environment alters the cuticular hydrocarbon composition of harvester ants. *Journal of Chemical Ecology, 27*(9), 1805–1819. https://doi.org/10.1023/A:1010408725464.

Wicker-Thomas, C., & Chertemps, T. (2010). Molecular biology and genetics of hydrocarbon production. In G. Blomquist, & A. Bagnères (Eds.), *Insect hydrocarbons: biology, biochemistry and chemical ecology* (pp. 53–74). Cambridge, U.K.: Cambridge University Press. https://doi.org/10.1017/CBO9780511711909.005.

Woodward, G., Benstead, J. P., Beveridge, O. S., Blanchard, J., Brey, T., Brown, L. E., et al. (2010). Ecological networks in a changing climate. *Advances in Ecological Research, 42*, 71–138. https://doi.org/10.1016/B978-0-12-381363-3.00002-2.

Zweden, J. S. Van, Dreier, S., & d'Ettorre, P. (2009). Disentangling environmental and heritable nestmate recognition cues in a carpenter ant. *Journal of Insect Physiology, 55*, 159–164. https://doi.org/10.1016/j.jinsphys.2008.11.001.

Appendix

Aphaenogaster iberica Cytochrome Oxidase I (COI) Primer Sequences

Primers AibCOIF 5′-TAATTATCCGCTTAGAATTAGG-3′ and AibCOIR 5′-AAATGTTGGGGAAAGAAAGT-3' were used to amplify mitochondrial COI sequences at Tm: 52 °C.

Microsatellite Genotyping

Each pair of primers was 5' labelled with the fluorescent dyes 6-FAM, NED, VIC or PET. Genomic DNA was extracted using the Wizard Genomic DNA Purification Kit (Promega). PCR amplification was carried out using multiplex reactions, which contained 0.5 U of Taq DNA polymerase, 6 pmol of dNTP, 37.5 pmol of $MgCl_2$ and oligonucleotides listed in Table A2. The multiplex PCR thermal cycle was as follows: 10 min at 95C followed by 40 cycles of 95C for 45 s, 56C annealing for 1 min and 72C extension for 1 min 30 s, with a final 10 min extension step at 72 °C. One μl of each multiplex product or a 1/10 dilution of the PCR products was subjected to capillary electrophoresis, which was performed with an ABI 3730 XL (Applied Biosystems) sequencer with the LIZ500 standard (Applied Biosystems). The following migration conditions were used: injection time: 15 s; run voltage: 15 kV; run time: 1600 s. Allele scoring was performed using Geneious v. 8.0.3.

Table A1
Sampling locations and NCBI data accession information for the *A. iberica* COI sequences

Sequence ID	Country	GPS coordinates	Specimen voucher	NCBI accession number
Z100_01	Spain	N36° 46.7046 W3° 33.2112	AiA01	MK160258
Z100_02	Spain	N36° 46.7412 W3° 33.2136	AiA02	MK160259
Z100_03	Spain	N36° 46.7724 W3° 33.3882	AiA03	MK160260
Z100_04	Spain	N36° 46.7544 W3° 33.3858	AiA04	MK160261
Z100_05	Spain	N36° 46.6908 W3° 33.1974	AiA05	MK160262
Z100_06	Spain	N36° 46.6788 W3° 33.2568	AiA06	MK160263
Z100_07	Spain	N36° 46.6998 W3° 33.2532	AiA07	MK160264
Z100_08	Spain	N36° 46.905 W3° 33.0162	AiA08	MK160265
Z100_09	Spain	N36° 46.7118 W3° 33.2022	AiA09	MK160266
Z100_10	Spain	N36° 46.7046 W3° 33.2112	AiA10	MK160267
Z100_11	Spain	N36° 46.7082 W3° 33.195	AiA11	MK160268
Z100_12	Spain	N36° 46.7064 W3° 33.2058	AiA12	MK160269
Z100_13	Spain	N36° 46.755 W3° 33.1824	AiA13	MK160270
Z100_14	Spain	N36° 46.7334 W3° 33.2244	AiA14	MK160271
Z100_15	Spain	N36° 46.7952 W3° 33.1518	AiA15	MK160272
Z100_16	Spain	N36° 46.71 W3° 33.2262	AiA16	MK160273
Z100_17	Spain	N36° 46.7406 W3° 33.195	AiA17	MK160274
Z100_18	Spain	N36° 46.728 W3° 33.2022	AiA18	MK160275
Z100_19	Spain	N36° 46.7076 W3° 33.2514	AiA19	MK160276
Z100_20	Spain	N36° 46.7082 W3° 33.2448	AiA20	MK160277
Z100_21	Spain	N36° 46.6872 W3° 33.2604	AiA21	MK160278
Z100_22	Spain	N36° 46.7148 W3° 33.2298	AiA22	MK160279
Z100_23	Spain	N36° 46.6854 W3° 33.249	AiA23	MK160280
Z100_24	Spain	N36° 46.7106 W3° 33.213	AiA24	MK160281
Z100_25	Spain	N36° 46.704 W3° 33.2172	AiA25	MK160282
Z100_26	Spain	N36° 46.6884 W3° 33.2628	AiA26	MK160283
Z100_27	Spain	N36° 46.7004 W3° 33.2178	AiA27	MK160284
Z100_28	Spain	N36° 46.6776 W3° 33.2538	AiA28	MK160285
Z100_29	Spain	N36° 46.7202 W3° 33.2874	AiA29	MK160286
Z100_30	Spain	N36° 46.7046 W3° 33.2268	AiA30	MK160287
Z100_31	Spain	N36° 46.7226 W3° 33.3006	AiA31	MK160288
Z150_01	Spain	N36° 48.9426 W3° 32.5566	AiH01	MK160289
Z150_02	Spain	N36° 48.9486 W3° 32.538	AiH02	MK160290
Z150_03	Spain	N36° 48.9504 W3° 32.547	AiH03	MK160291
Z150_04	Spain	N36° 48.9636 W3° 32.5428	AiH04	MK160292
Z150_05	Spain	N36° 48.9846 W3° 32.5386	AiH05	MK160293
Z150_06	Spain	N36° 48.9888 W3° 32.547	AiH06	MK160294
Z150_07	Spain	N36° 48.993 W3° 32.5476	AiH07	MK160295
Z150_08	Spain	N36° 48.9996 W3° 32.5506	AiH08	MK160296

(*continued on next page*)

Table A1 (*continued*)

Sequence ID	Country	GPS coordinates	Specimen voucher	NCBI accession number
Z150_09	Spain	N36° 49.002 W3° 32.5524	AiH09	MK160297
Z150_10	Spain	N36° 49.0062 W3° 32.5536	AiH10	MK160298
Z150_11	Spain	N36° 49.0188 W3° 32.5524	AiH11	MK160299
Z150_12	Spain	N36° 49.0272 W3° 32.5482	AiH12	MK160300
Z150_13	Spain	N36° 49.0308 W3° 32.547	AiH13	MK160301
Z150_14	Spain	N36° 49.0392 W3° 32.5416	AiH14	MK160302
Z150_15	Spain	N36° 49.041 W3° 32.5404	AiH15	MK160303
Z150_16	Spain	N36° 49.041 W3° 32.5404	AiH16	MK160304
Z150_17	Spain	N36° 49.071 W3° 32.5248	AiH17	MK160305
Z150_18	Spain	N36° 49.0692 W3° 32.5296	AiH18	MK160306
Z150_19	Spain	N36° 49.0722 W3° 32.5296	AiH19	MK160307
Z150_20	Spain	N36° 49.0746 W3° 32.5296	AiH20	MK160308
Z150_21	Spain	N36° 49.083 W3° 32.5254	AiH21	MK160309
Z150_22	Spain	N36° 49.05 W3° 32.5254	AiH22	MK160310
Z150_23	Spain	N36° 49.0926 W3° 32.5176	AiH23	MK160311
Z150_24	Spain	N36° 49.1028 W3° 32.5044	AiH24	MK160312
Z150_26	Spain	N36°49.0788 W3°32.5320	AiH25	–
Z150_26	Spain	N36° 49.056 W3° 32.5344	AiH26	MK160313
Z150_27	Spain	N36° 48.9852 W3° 32.5422	AiH27	MK160314
Z150_28	Spain	N36° 48.9888 W3° 32.5428	AiH28	MK160315
Z150_29	Spain	N36° 48.957 W3° 32.541	AiH29	MK160316
Z150_30	Spain	N36° 48.9444 W3° 32.535	AiH30	MK160317
Z300_01	Spain	N36° 51.8172 W3° 29.9502	AiG01	MK160318
Z300_02	Spain	N36° 51.8238 W3° 29.949	AiG02	MK160319
Z300_03	Spain	N36° 51.8256 W3° 29.952	AiG03	MK160320
Z300_04	Spain	N36° 51.8184 W3° 29.9538	AiG04	MK160321
Z300_05	Spain	N36° 51.822 W3° 29.9616	AiG05	MK160322
Z300_06	Spain	N36° 51.8238 W3° 29.964	AiG06	MK160323
Z300_07	Spain	N36° 51.8208 W3° 29.9646	AiG07	MK160324
Z300_08	Spain	N36° 51.819 W3° 29.967	AiG08	MK160325
Z300_09	Spain	N36° 51.816 W3° 29.9652	AiG09	MK160326
Z300_10	Spain	N36° 51.813 W3° 29.9622	AiG10	MK160327
Z300_11	Spain	N36° 51.8094 W3° 29.9616	AiG11	MK160328
Z300_12	Spain	N36° 51.8088 W3° 29.9532	AiG12	MK160329
Z300_13	Spain	N36° 51.8112 W3° 29.9514	AiG13	MK160330
Z300_14	Spain	N36° 51.8064 W3° 29.9394	AiG14	MK160331
Z300_15	Spain	N36° 51.7968 W3° 29.9286	AiG15	MK160332
Z300_16	Spain	N36° 51.792 W3° 29.9238	AiG16	MK160333
Z300_17	Spain	N36° 51.795 W3° 29.9262	AiG17	MK160334
Z300_18	Spain	N36° 51.813 W3° 29.9556	AiG18	MK160335
Z300_19	Spain	N36° 51.8292 W3° 29.9712	AiG19	MK160336
Z300_20	Spain	N36° 51.8358 W3° 29.9694	AiG20	MK160337
Z300_21	Spain	N36° 51.852 W3° 29.9928	AiG21	MK160338
Z300_22	Spain	N36° 51.8556 W3° 29.9952	AiG22	MK160339
Z300_23	Spain	N36° 51.8622 W3° 30.0024	AiG23	MK160340
Z300_24	Spain	N36° 51.816 W3° 29.9322	AiG24	MK160341
Z300_25	Spain	N36° 51.816 W3° 29.9436	AiG25	MK160342
Z600_01	Spain	N36° 54.594 W3° 30.7626	AiB01	MK160343
Z600_02	Spain	N36° 54.5814 W3° 30.7476	AiB02	MK160344
Z600_03	Spain	N36° 54.5616 W3° 30.7488	AiB03	MK160345
Z600_04	Spain	N36° 54.5754 W3° 30.7356	AiB04	MK160346
Z600_05	Spain	N36° 54.5754 W3° 30.7152	AiB05	MK160347
Z600_06	Spain	N36° 54.6096 W3° 30.7146	AiB06	MK160348
Z600_07	Spain	N36° 54.5922 W3° 30.6798	AiB07	MK160349
Z600_08	Spain	N36° 54.5772 W3° 30.6798	AiB08	MK160350
Z600_09	Spain	N36° 54.5622 W3° 30.735	AiB09	MK160351
Z600_10	Spain	N36° 54.6012 W3° 30.7212	AiB10	MK160352
Z600_11	Spain	N36° 54.6012 W3° 30.7422	AiB11	MK160353
Z600_12	Spain	N36° 54.612 W3° 30.7518	AiB12	MK160354
Z600_13	Spain	N36° 54.612 W3° 30.639	AiB13	MK160355
Z600_14	Spain	N36° 54.6498 W3° 30.6186	AiB14	MK160356
Z600_15	Spain	N36° 54.5994 W3° 30.7086	AiB15	MK160357
Z600_16	Spain	N36° 54.633 W3° 30.7824	AiB16	MK160358
Z600_17	Spain	N36° 54.6306 W3° 30.6942	AiB17	MK160359
Z600_18	Spain	N36° 54.627 W3° 30.603	AiB18	MK160360
Z600_19	Spain	N36° 54.591 W3° 30.6894	AiB19	MK160361
Z600_20	Spain	N36° 54.6228 W3° 30.6	AiB20	MK160362
Z600_21	Spain	N36° 54.6426 W3° 30.5886	AiB21	MK160363
Z600_22	Spain	N36° 54.6414 W3° 30.5886	AiB22	MK160364
Z600_23	Spain	N36° 54.618 W3° 30.579	AiB23	MK160365
Z600_24	Spain	N36° 54.6276 W3° 30.5814	AiB24	MK160366
Z600_25	Spain	N36° 54.681 W3° 30.6258	AiB25	MK160367
Z600_26	Spain	N36° 54.597 W3° 30.735	AiB26	MK160368
Z600_27	Spain	N36° 54.5802 W3° 30.747	AiB27	MK160369
Z600_28	Spain	N36° 54.5796 W3° 30.753	AiB28	MK160370
Z600_29	Spain	N36° 54.6198 W3° 30.6096	AiB29	MK160371
Z600_30	Spain	N36° 54.6138 W3° 30.591	AiB30	MK160372

Table A1 (*continued*)

Sequence ID	Country	GPS coordinates	Specimen voucher	NCBI accession number
Z1000_01	Spain	N36° 56.0076 W3° 30.2736	AiC01	MK160373
Z1000_02	Spain	N36° 56.004 W3° 30.318	AiC02	MK160374
Z1000_03	Spain	N36° 56.0088 W3° 30.3438	AiC03	MK160375
Z1000_04	Spain	N36° 55.9836 W3° 30.273	AiC04	MK160376
Z1000_05	Spain	N36° 56.0064 W3° 30.2556	AiC05	MK160377
Z1000_06	Spain	N36° 56.0208 W3° 30.2688	AiC06	MK160378
Z1000_07	Spain	N36°56.0124 W3°30.2760	AiC07	–
Z1000_08	Spain	N36° 56.0412 W3° 30.309	AiC08	MK160379
Z1000_09	Spain	N36° 56.031 W3° 30.2802	AiC09	MK160380
Z1000_10	Spain	N36° 56.046 W3° 30.3402	AiC10	MK160381
Z1000_11	Spain	N36° 56.0412 W3° 30.2622	AiC11	MK160382
Z1000_12	Spain	N36° 55.98 W3° 30.2718	AiC12	MK160383
Z1000_13	Spain	N36° 55.9824 W3° 30.2664	AiC13	MK160384
Z1000_14	Spain	N36° 55.986 W3° 30.2688	AiC14	MK160385
Z1000_15	Spain	N36°55.9824 W3°30.2754	AiC15	–
Z1000_16	Spain	N36° 56.0166 W3° 30.2736	AiC16	MK160386
Z1000_17	Spain	N36° 56.0202 W3° 30.27	AiC17	MK160387
Z1000_18	Spain	N36° 56.013 W3° 30.273	AiC18	MK160388
Z1000_20	Spain	N36° 56.0088 W3° 30.3354	AiC20	MK160389
Z1000_21	Spain	N36° 55.989 W3° 30.2742	AiC21	MK160390
Z1000_22	Spain	N36° 55.9878 W3° 30.2574	AiC22	MK160391
Z1000_24	Spain	N36° 55.9926 W3° 30.2514	AiC24	MK160392
Z1000_25	Spain	N36° 55.9914 W3° 30.2616	AiC25	MK160393
Z1000_26	Spain	N36° 56.0154 W3° 30.2688	AiC26	MK160394
Z1000_27	Spain	N36° 56.0016 W3° 30.2742	AiC27	MK160395
Z1000_28	Spain	N36° 56.0154 W3° 30.276	AiC28	MK160396
Z1000_29	Spain	N36° 56.0178 W3° 30.2676	AiC29	MK160397
Z1000_30	Spain	N36° 56.007 W3° 30.2718	AiC30	MK160398
Z1000_31	Spain	N36° 56.0034 W3° 30.27	AiC31	MK160399
Z1000_32	Spain	N36° 56.0358 W3° 30.2196	AiC32	MK160400
Z1300_01	Spain	N36° 56.7552 W3° 29.8812	AiD01	MK160401
Z1300_02	Spain	N36° 56.748 W3° 29.8536	AiD02	MK160402
Z1300_03	Spain	N36° 56.748 W3° 29.8452	AiD03	MK160403
Z1300_04	Spain	N36° 56.7612 W3° 29.8806	AiD04	MK160404
Z1300_05	Spain	N36° 56.7546 W3° 29.916	AiD05	MK160405
Z1300_06	Spain	N36° 56.7534 W3° 29.964	AiD06	MK160406
Z1300_07	Spain	N36° 56.7162 W3° 29.9436	AiD07	MK160407
Z1300_08	Spain	N36° 56.7132 W3° 29.9232	AiD08	MK160408
Z1300_09	Spain	N36° 56.7336 W3° 29.9334	AiD09	MK160409
Z1300_10	Spain	N36° 56.736 W3° 29.9184	AiD10	MK160410
Z1300_11	Spain	N36° 56.772 W3° 29.9088	AiD11	MK160411
Z1300_12	Spain	N36° 56.7786 W3° 29.8884	AiD12	MK160412
Z1300_13	Spain	N36° 56.7474 W3° 29.9046	AiD13	MK160413
Z1300_14	Spain	N36° 56.6868 W3° 30.0126	AiD14	MK160414
Z1300_15	Spain	N36° 56.6526 W3° 30.03	AiD15	MK160415
Z1300_16	Spain	N36° 56.6754 W3° 29.9742	AiD16	MK160416
Z1300_17	Spain	N36° 56.6754 W3° 30.0372	AiD17	MK160417
Z1300_18	Spain	N36° 56.7036 W3° 29.9616	AiD18	MK160418
Z1300_19	Spain	N36° 56.7102 W3° 30.009	AiD19	MK160419
Z1300_20	Spain	N36° 56.7282 W3° 29.8968	AiD20	MK160420
Z1300_21	Spain	N36° 56.7552 W3° 29.88	AiD21	MK160421
Z1300_22	Spain	N36° 56.7552 W3° 29.9196	AiD22	MK160422
Z1300_23	Spain	N36° 56.7474 W3° 29.9094	AiD23	MK160423
Z1300_24	Spain	N36° 56.7396 W3° 29.9052	AiD24	MK160424
Z1300_25	Spain	N36° 56.754 W3° 29.9082	AiD25	MK160425
Z1300_26	Spain	N36° 56.7564 W3° 29.8908	AiD26	MK160426
Z1300_27	Spain	N36° 56.7576 W3° 29.889	AiD27	MK160427
Z1300_28	Spain	N36° 56.7588 W3° 29.8824	AiD28	MK160428
Z1300_29	Spain	N36° 56.7648 W3° 29.8878	AiD29	MK160429
Z1300_30	Spain	N36° 56.7462 W3° 29.8596	AiD30	MK160430
Z1700_01	Spain	N36° 56.9076 W3° 28.8036	AiE01	MK160431
Z1700_02	Spain	N36° 56.9148 W3° 28.7994	AiE02	MK160432
Z1700_03	Spain	N36° 56.9172 W3° 28.803	AiE03	MK160433
Z1700_04	Spain	N36° 56.9214 W3° 28.8012	AiE04	MK160434
Z1700_05	Spain	N36° 56.9016 W3° 28.8042	AiE05	MK160435
Z1700_06	Spain	N36° 56.91 W3° 28.8054	AiE06	MK160436
Z1700_07	Spain	N36° 56.9166 W3° 28.8096	AiE07	MK160437
Z1700_08	Spain	N36° 56.9166 W3° 28.8072	AiE08	MK160438
Z1700_09	Spain	N36° 56.9202 W3° 28.8054	AiE09	MK160439
Z1700_10	Spain	N36° 56.9232 W3° 28.8054	AiE10	MK160440
Z1700_11	Spain	N36° 56.8938 W3° 28.8432	AiE11	MK160441
Z1700_12	Spain	N36° 56.9226 W3° 28.797	AiE12	MK160442
Z1700_13	Spain	N36°56.9334 W3°28.8096	AiE13	–
Z1700_14	Spain	N36° 56.9256 W3° 28.8012	AiE14	MK160443
Z1700_15	Spain	N36° 56.871 W3° 28.803	AiE15	MK160444

(*continued on next page*)

Table A1 (*continued*)

Sequence ID	Country	GPS coordinates	Specimen voucher	NCBI accession number
Z1700_16	Spain	N36° 56.9172 W3° 28.7994	AiE16	MK160445
Z1700_17	Spain	N36° 56.9364 W3° 28.8072	AiE17	MK160446
Z1700_18	Spain	N36° 56.9316 W3° 28.8108	AiE18	MK160447
Z1700_19	Spain	N36° 56.9088 W3° 28.8132	AiE19	MK160448
Z1700_20	Spain	N36° 56.8926 W3° 28.8234	AiE20	MK160449
Z1700_21	Spain	N36° 56.8764 W3° 28.8006	AiE21	MK160450
Z1700_22	Spain	N36° 56.9226 W3° 28.7964	AiE22	MK160451
Z1700_23	Spain	N36° 56.9304 W3° 28.8018	AiE23	MK160452
Z1700_24	Spain	N36° 56.928 W3° 28.8018	AiE24	MK160453
Z1700_25	Spain	N36° 56.9076 W3° 28.794	AiE25	MK160454
Z1700_26	Spain	N36° 56.9286 W3° 28.8078	AiE26	MK160455
Z1700_27	Spain	N36° 56.904 W3° 28.815	AiE27	MK160456
Z1700_28	Spain	N36° 56.9328 W3° 28.7982	AiE28	MK160457
Z1700_29	Spain	N36° 56.88 W3° 28.797	AiE29	MK160458
Z1700_30	Spain	N36° 56.9142 W3° 28.803	AiE30	MK160459
Z2000_01	Spain	N36° 57.8622 W3° 29.0406	AiF01	MK160460
Z2000_02	Spain	N36° 57.861 W3° 29.0394	AiF02	MK160461
Z2000_03	Spain	N36° 57.8616 W3° 29.0328	AiF03	MK160462
Z2000_04	Spain	N36° 57.8598 W3° 29.031	AiF04	MK160463
Z2000_05	Spain	N36° 57.882 W3° 29.0484	AiF05	MK160464
Z2000_06	Spain	N36° 57.8826 W3° 29.0544	AiF06	MK160465
Z2000_07	Spain	N36° 57.8574 W3° 29.0364	AiF07	MK160466
Z2000_08	Spain	N36° 57.8598 W3° 29.0328	AiF08	MK160467
Z2000_09	Spain	N36° 57.864 W3° 29.0322	AiF09	MK160468
Z2000_10	Spain	N36° 57.8688 W3° 29.0256	AiF10	MK160469
Z2000_11	Spain	N36° 57.8484 W3° 29.04	AiF11	MK160470
Z2000_12	Spain	N36°57.8682 W3°29.0478	AiF12	–
Z2000_13	Spain	N36° 57.8532 W3° 29.0238	AiF13	MK160471
Z2000_14	Spain	N36° 57.846 W3° 29.0148	AiF14	MK160472
Z2000_15	Spain	N36° 57.8538 W3° 29.0184	AiF15	MK160473
Z2000_16	Spain	N36° 57.8976 W3° 29.0532	AiF16	MK160474
Z2000_17	Spain	N36° 57.8574 W3° 29.0232	AiF17	MK160475
Z2000_18	Spain	N36° 57.8556 W3° 29.0232	AiF18	MK160476
Z2000_19	Spain	N36° 57.8904 W3° 29.0508	AiF19	MK160477
Z2000_20	Spain	N36° 57.8682 W3° 29.0484	AiF20	MK160478
Z2000_21	Spain	N36° 57.8838 W3° 29.0454	AiF21	MK160479
Z2000_22	Spain	N36° 57.9042 W3° 29.0574	AiF22	MK160480
Z2000_23	Spain	N36° 57.8706 W3° 29.0502	AiF23	MK160481
Z2000_25	Spain	N36° 57.8784 W3° 29.0472	AiF25	MK160482
Z2000_28	Spain	N36° 57.912 W3° 29.061	AiF28	MK160483
Z2000_29	Spain	N36° 57.9204 W3° 29.0598	AiF29	MK160484
Z2000_30	Spain	N36° 57.8886 W3° 29.0556	AiF30	MK160485

Table A2
Primer concentration at each multiplex microsatellite PCR

Marker	pmol	Multiplex
Ant8498	2	1
Ant12220	5	
Ant8424	5	
Asen15	2	2
Ant2936	4	
Ant11893	4	
Ant7680	2	
Asen94	4	

Table A3
Linkage disequilibrium tests for the microsatellite markers

Locus pairs	χ^2	*df*	*P*
Asen15 vs Ant2936	15.70	16	0.47
Asen15 vs Ant11893	15.63	16	0.47
Ant2936 vs Ant11893	12.71	16	0.69
Asen15 vs Ant7680	18.35	16	0.30
Ant2936 vs Ant7680	22.03	16	0.14
Ant11893 vs Ant7680	14.16	16	0.58
Asen15 vs Asen94	9.91	16	0.87
Ant2936 vs Asen94	10.96	16	0.81
Ant11893 vs Asen94	6.99	16	0.97
Ant7680 vs Asen94	24.81	16	0.07
Asen15 vs Ant8498	44.12	16	0.0001
Ant2936 vs Ant8498	Infinity	16	<0.0001
Ant11893 vs Ant8498	23.97	16	0.08
Ant7680 vs Ant8498	15.76	16	0.46
Asen94 vs Ant8498	13.18	16	0.65
Asen15 vs Ant12220	14.59	14	0.40
Ant2936 vs Ant12220	12.47	14	0.56
Ant11893 vs Ant12220	6.04	14	0.96
Ant7680 vs Ant12220	11.62	14	0.63
Asen94 vs Ant12220	6.36	14	0.95
Ant8498 vs Ant12220	9.86	14	0.77
Asen15 vs Ant842	10.31	16	0.84
Ant2936 vs Ant8424	13.19	16	0.65
Ant11893 vs Ant8424	18.92	16	0.27
Ant7680 vs Ant8424	4.66	16	0.99
Asen94 vs Ant8424	11.99	16	0.74
Ant8498 vs Ant8424	3.06	16	0.99
Ant12220 vs Ant8424	4.73	14	0.98

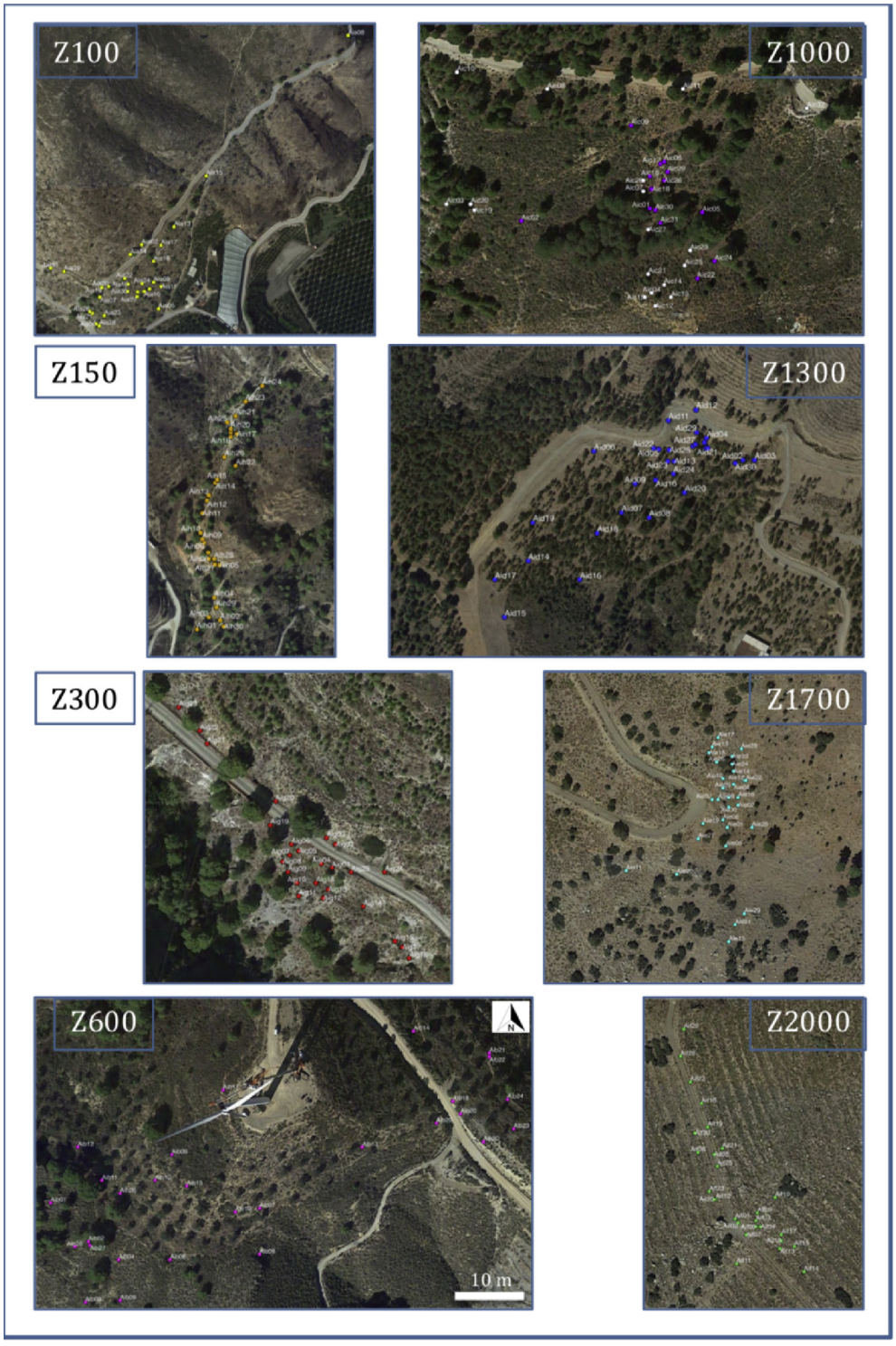

Figure A1. Locations of the *Aphaenogaster iberica* colonies used in the genetic analyses.